IC/90/199

INTERNATIONAL CENTRE FOR THEORETICAL PHYSICS

GLUON ASYMMETRIES IN THE LEPTOPRODUCTION OF J/ψ

R.M. Godbole

Sourendu Gupta

and

K. Sridhar

INTERNATIONAL ATOMIC ENERGY AGENCY

UNITED NATIONS EDUCATIONAL, SCIENTIFIC AND CULTURAL ORGANIZATION

1990 MIRAMARE - TRIESTE

IC/90/199

International Atomic Energy Agency
and
United Nations Educational Scientific and Cultural Organization
INTERNATIONAL CENTRE FOR THEORETICAL PHYSICS

GLUON ASYMMETRIES IN THE LEPTOPRODUCTION OF J/ψ *

R.M. Godbole **
International Centre for Theoretical Physics, Trieste, Italy,

Sourendu Gupta
Fakultät für Physik, Universität Bielefeld, D-4800 Bielefeld 1, Federal Republic of Germany

and

K. Sridhar
Department of Physics, University of Bombay, Kalina, Bombay 400 098, India.

ABSTRACT

We study J/ψ production, in deep inelastic scattering experiments with polarised beams and polarised targets. The spin asymmetries are seen to depend strongly on the particular form of the spin dependent gluon distributions used. Therefore, it should be possible in these experiments, to discriminate between different parametrizations of polarised gluon distributions, and hence between the distinctly different physical pictures of the proton spin underlying these parametrizations.

MIRAMARE – TRIESTE
July 1990

* To be submitted for publication.
** Permanent address: Department of Physics, University of Bombay, Kalina, Bombay 400 098, India.

The measurement in polarised lepton-proton deep inelastic scattering [1,2] of the asymmetry, A_1^p, given by

$$A_1^p(x,Q^2) = \frac{2xg_1^p(x,Q^2)}{F_2^p(x,Q^2)} \tag{1}$$

has provided some new information on the spin structure of the proton. Here $F_2^p(x,Q^2)$ is the unpolarised structure function whereas $g_1^p(x,Q^2)$ is the polarised structure function of the proton, *i.e.*

$$F_2^p(x,Q^2) = x\sum_q e_q^2[q(x,Q^2)+\bar{q}(x,Q^2)] \tag{2}$$

$$g_1^p(x,Q^2) = \frac{1}{2}\sum[\Delta q(x,Q^2)+\Delta\bar{q}(x,Q^2)] \tag{3}$$

where $q(\bar{q})$ is the usual unpolarised distribution and $\Delta q(\Delta\bar{q})$ is its polarised counterpart. These may be expressed in terms of $q_+(q_-)$ which are the parton distributions of flavour q aligned (anti-aligned) with the proton spin as

$$q(x,Q^2) \equiv q_+ + q_- \qquad \Delta q(x,Q^2) \equiv q_+ - q_- \tag{4.a}$$

$$\bar{q}(x,Q^2) \equiv \bar{q}_+ + \bar{q}_- \qquad \Delta\bar{q}(x,Q^2) \equiv \bar{q}_+ - \bar{q}_- \tag{4.b}$$

Experimental measurements of the asymmetry provide us with a determination of $g_1^p(x,Q^2)$. Writing $g_1^p(Q^2) \equiv \int_0^1 g_1^p(x,Q^2)dx$ as

$$g_1^p(Q^2) = \frac{1}{2}[\frac{4}{9}\Delta u(Q^2) + \frac{1}{9}\Delta d(Q^2) + \frac{1}{9}\Delta s(Q^2)] \tag{5}$$

and using the F/D ratio of the hyperon decay and the Bjorken sum rule, the following values for the first moments of the polarised density functions of the quarks have been obtained [3]

$$\Delta u = 0.73 \pm 0.07 \tag{6.a}$$

$$\Delta d = -0.52 \pm 0.07 \tag{6.b}$$

$$\Delta s = -0.22 \pm 0.07 \tag{6.c}$$

which gives the total spin carried by the quarks to be

$$\Delta q = \Delta u + \Delta d + \Delta s \simeq -0.01 \pm 0.21 \tag{7}$$

implying that the net spin carried by the quarks is almost zero.

The total polarisation Δq measures the $SU(3)$ singlet axial current in the leading order. Corrections to these come from higher order diagrams where the quark in a proton radiates a gluon. Naively, one would expect these higher order contributions to be suppressed. However, due to the axial anomaly, the gluon contribution is not suppressed and the first moment of the singlet part of g_1^p recieves order α_s^0 contribution from the gluon asymmetry [4]. Therefore the moments measured in the experiment are not Δq, but

$$\Delta\tilde{q} = \Delta q - \frac{\alpha_s}{2\pi}\Delta G \tag{8}$$

where $\Delta G = G_+(x, Q^2) - G_-(x, Q^2)$ with $G_{+(-)}$ denoting the distributions of the gluons with spins aligned parallel(anti-parallel) to the proton. If the gluon asymmetry is large and positive then it can compensate the quark contribution so that $\Delta\tilde{q}$ is small. Thus in this picture, the gluon could carry a large part of the proton spin. We note here that the vanishing of the singlet axial current matrix element is not *explained* by this mechanism, whereas in the context of the Skyrme model, using the $1/N_C$ approximation, it has been shown that this matrix element as well as the first moment of the gluon distribution function is zero. Therefore, in this picture the net spin of the proton would have to be associated with the relative angular momentum between the partons. An independent determination of the gluon spin densities then becomes crucial in the understanding of the spin structure of the proton [3,5]. This will serve to determine the contribution of the gluon to the proton spin and help decide whether other contributions such as large strange quark asymmetry or relative orbital angular momentum between the partons are important.

In this paper, we study a process which can, in principle, yield invaluable information on spin-dependent gluon densities, and hence help clarify the physical picture of proton spin *viz.* J/ψ production in polarised lepton-proton scattering. This we do using various parametrisations of the gluon spin distributions which are consistent with the constraints from the EMC experiment. Recent studies of photoproduction[6] and leptoproduction [5,7] of open charm have been considered in the literature. Photoproduction of J/ψ has been discussed in Ref. [8]. J/ψ production which provides a better experimental signal than

open $c\bar{c}$ production, has also been considered in Ref. [6]. In the present work we make a detailed study of the dependence of polarised J/ψ production on various parametrisations of polarised gluon distributions consistent with the EMC data. Our aim will be to find out if the predictions due to the different parametrisations are sufficiently different to be discriminated in experiment. Thus, the information from J/ψ production experiments can be used to constrain the various models of proton spin.

Photoproduction and leptoproduction of J/ψ probes the gluon distributions at small values of x (e.g. for photoproduction, $x \approx m^2_{J/\psi}/s_{\gamma p}$, where $s_{\gamma p}$ is the photon-nucleon centre-of-mass energy. The advantage of using these processes in studying spin-dependent gluon densities is that the asymmetry is likely to be large at these values. Further, in leptoproduction, it is possible to choose Q^2 values in such a way that we can get a handle on polarised gluon distributions over a range of x values. We consider the scattering of a polarised lepton from a polarised proton giving rise to a $c\bar{c}$ pair in the final state,

$$lp \to l(c\bar{c})X \tag{9}$$

through what is called photon-gluon fusion:

$$\gamma g \to c\bar{c} \tag{10}$$

The cross-section is calculated by producing $c\bar{c}$ pairs with invariant mass m^2 in the range $4m_c^2 \leq m^2 \leq 4m_D^2$. To obtain the J/ψ cross section from the $c\bar{c}$ cross section we use the semi-local duality approach [9]. The hypothesis, known as semi-local duality, is that this cross-section integrated over the given mass-range will be the sum of the cross-sections of all the $c\bar{c}$ bound states in this range. The J/ψ cross-section is then obtained by dividing by the total number of resonances. Even though the normalisation is not a good prediction of this model, the shapes of the distributions are seen to be reproduced well for the case of unpolarised J/ψ production [10], in the elastic region, $z \geq 0.95$,with z defined by

$$z = E_{J/\psi}/E_\gamma \tag{11}$$

where $E_{J/\psi}$ and E_γ are the lab energies of the J/ψ and the virtual photon respectively. We note that there exists an alternate model for J/ψ production – the colour singlet model [11]. In this model the $c\bar{c}$ is explicitly constructed to be a colour singlet by radiating a hard gluon in the final state. This model is applicable only to *inelastic* J/ψ production. Since we are interested in the elastic case, we consider only the semi-local duality approach.

The process $lp \to l(c\bar{c})X$ with polarised beam and polarised target has been discussed earlier [12,13]. The virtual photon emitted by the polarised lepton is in a state which is a linear superposition of a transverse elliptical and a longitudinal polarisation state [14]. The components of the 'virtual photon polarisation vector ' given by

$$\epsilon_\mu = \frac{1}{(2Q^2)^{\frac{1}{2}}} \bar{u}(l_2)\gamma_\mu u(l_1) \tag{12}$$

(where l_1 and l_2 are the momenta of the incoming and the outgoing lepton, and Q^2 the invariant mass of the virtual photon) are evaluated using the leptonic tensor $L_{\mu\nu}$ and are expressed in terms of a polarisation parameter ϵ, where

$$\epsilon = \frac{L_{xx} - L_{yy}}{L_{xx} + L_{yy}} \tag{13}$$

The parameter ϵ measures the magnitude of the transverse linear polarisation of the virtual photon. In terms of the beam energy, E, the photon energy, ν, and Q^2, ϵ may be written as

$$\epsilon = \frac{4E(E-\nu) - Q^2}{4E(E-\nu) + Q^2 + 2\nu^2} \tag{14}$$

which in turn gives,

$$\epsilon^{-1} = 1 + \frac{2q_3^2}{Q^2} tan^2 \frac{\theta}{2} \tag{15}$$

Here $q_3^2 = Q^2 + \nu^2$ and θ refers to the angle between the incident and outgoing lepton directions in the laboratory frame. The photon direction is taken to define the positive z-axis, the x-z plane is taken to to be the plane containing the incident and the final leptons, and ϕ is the angle between the lepton plane and the production plane containing the $c\bar{c}$ pair.

The differential cross-section written as a function of Q^2 and ν, after integrating over ϕ is given in Ref. [12], for helicities λ_g and λ_μ of the gluon and the muon respectively,

$$\frac{d\sigma_{\lambda_g\lambda_\mu}}{dQ^2 d\nu} = \frac{\alpha_s(Q_0^2)\alpha^2}{8\pi S Q^2 E\nu m_p} \int G(x, Q_0^2) \frac{|M|^2}{[\hat{s} + Q^2]} d\hat{s} \tag{16}$$

with

$$\begin{aligned} |M|^2 = & \frac{1}{(1-\epsilon)} \Bigg\{ \left[\frac{16m^2}{D} \beta(Q^2 - 2m^2) + \left[\frac{16m^4(3+\beta^2)}{D} - 8m^2 \right] \chi \right] \\ & + 2\lambda_g\lambda_\mu \frac{(1-\epsilon^2)^{\frac{1}{2}}}{(1-\beta^2)} \left[4m^2(1 - \frac{Q^2}{\hat{s}})\chi - 12\beta m^2 + Q^2\beta(1-\beta^2) \right] \\ & + \frac{4\epsilon Q^2}{D} \left[12m^2\beta - 2m^2(3-\beta^2)\chi \right] - \frac{4Q^2(1-\epsilon)}{D} \\ & \left[2m^2(1+\beta^2)\chi - 4m^2\beta \right] + \frac{2D}{(1-\beta^2)}(\chi - \beta) \Bigg\} \end{aligned} \tag{17}$$

where $D = \frac{4m^2}{\hat{s}}[\hat{s} + Q^2]$ and $\chi = ln[\frac{1+\beta}{1-\beta}]$. The asymmetry is defined as

$$A = \frac{d\sigma_{++} - d\sigma_{+-}}{d\sigma_{++} + d\sigma_{+-}} \tag{18}$$

where $+, -$ denote the values of λ_g and λ_μ in the above expression for the cross-section.

We use four different parametrisations of polarised gluon densities, $\Delta g(x)$, and compare their predictions for the asymmetries in J/ψ leptoproduction. The first two parametrisations for $\Delta g(x)$ that we use are from Ref. [15]. The two sets differ in their choice of unpolarised densities which are taken to be the EHLQ [16] and EMC [17] densities respectively. $\Delta g(x)$ is assumed to be proportional to $g(x)$ and the parametrisations for $\Delta g(x)$ and $g(x)$ are as follows:

For Set I with EHLQ unpolarised densities:

$$xg(x) = 2.62(1 + 3.5x)(1-x)^{5.9} \tag{19.a}$$

$$x\Delta g(x) = N_g x^\alpha (1 + ax)(1-x)^{5.9} \tag{19.b}$$

The values of α and a in the above equation for Δg are fixed using the positivity constraint

$$|\Delta g(x)| \le |g(x)| \tag{20}$$

For the second set using the EMC unpolarised densities (Set 2), we have

$$xg(x) = 4.548(1-x)^{7.5} \tag{21.a}$$

$$x\Delta g(x) = N_g x^\alpha (1-x)^{7.5} \tag{21.b}$$

with $\alpha = 0.25$ and $N_g = 3.186$. A third set of polarised gluon parametrisations (Set 3) taken from Ref. [18] is obtained by considering

$$\int_{0.1}^{1} g(x, Q^2 = 10\text{GeV}^2) \sim 1.5 \tag{22}$$

and taking $\Delta g(x)/g(x)$ to be small for large Q^2 and $x \to 0$. The parametrisations are then given as

$$\Delta g(x)/g(x) = 2(n+1)x(1-x)^n \tag{23}$$

with $n = 10$ and using unpolarised gluon densities from EHLQ [16] (set 2, $\Lambda = 290 MeV$ and $Q^2 = 100\text{GeV}^2$). The fourth set of polarised gluon densities (Set 4) that we consider are from Ref. [6], where at a value of $Q_0^2 = 4\text{GeV}^2, \Delta s$ is taken to be zero. That is, at this value of Q^2 the entire spin of the proton is assumed to be carried by the valence quarks and gluons. Assuming a form for the polarised valence quark distributions, the polarised gluon distributions are chosen in a such a way that the data from EMC on $g_1^p(x)$ is fitted. We have, then,

$$\Delta g(x) = Ax^{-0.3}(1-x)^7 \tag{24}$$

with $\int_0^1 \Delta g = 5.0$ and $Q_0^2 = 4\text{GeV}^2$. We have not considered the Q^2 evolution of the polarised densities but since the scale for this process is set around J/ψ production threshold, it is roughly equal to $m^2_{J/\psi}$. Hence we perform our computations using polarised densities at a fixed scale, Q_0^2.

In Fig. 1 we have plotted the gluon asymmetry, $\Delta g(x)/g(x)$ as a function of x for the different gluon parametrisations metioned above. For a lepton beam energy of 250 GeV (corresponding to the muon energy in the planned Spin Muon Collaboration (SMC) experiment with polarised muon beams and polarised proton target), we find, by varying Q^2 between 0.1 and 20.0 GeV^2 and ν between 70 and 190 GeV, that the values of x probed lie between 0.032 and 0.239. This band of allowed x-values is shown in Fig. 1. From Fig. 1 it is clear that all the parametrisations will predict a measurably large asymmetry for the values of x being probed in J/ψ leptoproduction. Further, the differences between the different parametrisations show up rather strikingly in this plot of $\Delta g(x)/g(x)$. In Fig. 2 we show the predictions of the parametrisations for the asymmetry at a lepton beam energy of 250 GeV. As we had anticipated the asymmetries are large and there is considerable difference between the predictions of the different parametrisations. The

parametrisation of polarised gluon densities of Set 4 predict consistently larger asymmetries than the other parametrisations. In particular, at large ν and large Q^2 ($\nu = 150 - 190$GeV and $Q^2 = 10 - 20$ GeV^2), the asymmetries are as large as -0.5 to -0.7. The cross-sections at such large values of ν and Q^2 are, however, correspondingly smaller. The cross-sections go down by an order of magnitude as we go from $\nu = 70$ GeV to $\nu = 190$ GeV at fixed Q^2, and by three orders of magnitude as we go from $Q^2 = 0.1$ GeV^2 to $Q^2 = 20.0$ GeV^2. This is likely to increase the error on the experimentally measured asymmetries making it somewhat difficult to discriminate between the predictions of different models of polarised gluon densities.

In Figs. 3 (a) and 3(b), we compare the predictions of Set 1 and Set 3, and Set 1 and Set 4 respectively. In the model of Set 1, there is some freedom in the choice of a, α and N_g. In Fig. 4, we have shown the predictions for the asymmetry for $\nu = 130 GeV$ using Set 1 parametrisations with values of the parameters chosen as given in Table 1.

TABLE 1

a	α	N_g
2.850	0.35	2.901
0.772	0.55	6.655
3.545	0.35	2.594
-0.606	1.00	29.891

a, α and N_g in the parametrisation of Set 1.

The smear due to these various choices becomes significant with increasing Q^2. The prediction of the first three choices given in Table 1 are not very different from each other, but the last choice with the negative a predicts asymmetries almost twice as large as the other three parametrisations. For comparison with other models we choose the values $\alpha = 0.35$, $a = 2.85$ and $N_g = 2.901$.

In conclusion, we would like to state the following : Leptoproduction of J/ψ using polarised lepton beams and polarised proton targets can be a very useful source of information on polarised gluon densities. Since the values of x probed by this experiment lie in the region where the gluon asymmetry is likely to be large, the resultant asymmetry measured in the experiment is also likely to be large. Leptoproduction of J/ψ offers more freedom than photoproduction experiments because the kinematics can be tuned to probe regions of phase space where gluon asymmetries are large and measurable. The data can be used to put constraints on the magnitude and the x-dependence of the gluon asymmetry, and can be used to discriminate between the various parametrisations of polarised structure functions and hence between the distinctly different physical pictures of the proton spin underlying these parametrisations,.

Acknowledgements: This work was partially supported by the Board of Research in Nuclear Sciences, India. The authors would like to thank the organisers of the Workshop in High Energy Phenomenology (1989), Tata Institute of Fundamental Research, Bombay, India, for providing a platform for discussion which led to the present paper. It is a pleasure to acknowledge interesting discussions with J. Pasupathy. One of us (S.K.) would like to acknowledge a research fellowship from the University Grants Commission, India. R.M.G. wishes to thank Professor Abdus Salam, the International Atomic Energy Agency and UNESCO for hospitality at the International Centre for Theoretical Physics, Trieste, where this work was completed and the Swedish Agency for Research Cooperation with Developing Countries, SAREC, for financial support during his visit at the ICTP under the Associateship scheme.

References:

[1] J. Ashman *et al.*, Phys. Lett. 206 B (1988), 364.

[2] G. Baum *et al.*, Phys. Rev. Lett. 51 (1983), 1135.

[3] E. Reya, "Spin Effects in Perturbative QCD", Talk presented at the XII th Warsaw Symposium in Elementary Particle Physics at Kazimierz (Poland) (29th May - 5th June 89) DO-TH-89/15. (To appear in the proceedings to be published by World Scientific)

[4] G. Altarelli and G.G. Ross, Phys. Lett. 212 B (1988), 391; R.D. Carlitz, J. Collins and A.H. Muller, Pittsburgh preprint 40423-11-P8 (1988).

[5] J. Ellis *et al.*, CERN Preprint CERN-TH-5471/89.

[6] G. Altarelli and W.J. Stirling, Particle World 1 (1989), 40.

[7] M. Glück and E. Reya, Z. Phys 39 C (1988), 569.

[8] P. Kalyniak, M.K. Sundaresan and J.S. Watson, Phys. Lett. 96 B, (1980), 184 .

[9] M. Glück and E. Reya, Phys. Lett. 79 B, (1978), 453; L. Jones and W. Wyld, Phys. Rev. D 17, (1978), 2332; J.P. Leveille and T. Weiler, Nucl. Phys. 147, (1979), 147; D.W. Duke and J.F. Owens, Phys. Lett. 96 B, (1980), 184.

[10] J.J. Aubert *et. al.* Nucl. Phys. B 203, (1983), 1.

[11] M.B. Einhorn and S.D. Ellis, Phys. Rev. D 12, (1975), 2007; M.B. Einhorn, S.D. Ellis and C. Quigg, Phys. Rev. Lett. 36, (1978), 1263; E.L. Berger and D. Jones, Phys. Rev. D 23, (1981), 1521; R. Baier and R. Rückl, Phys. Lett. 102 B, (1981), 364.

[12] A.D. Watson, Z. Phys 12 C (1982), 123.

[13] J.P. Guillet, Z. Phys 39 C (1988), 75.

[14] N. Dombey, Rev. Mod. Phys. 41, (1969)

[15] S. Gupta, J. Pasupathy, C. Swezd, Z. Phys 46 C (1990), 111 .

[16] E. Eichten *et al.*, Rev. Mod. Phys. 56 (1984) 579.

[17] T. Sloan *et al.*, Phys. Rep. 162 C (1988) 45.

[18] Z. Kunzst, Phys. Lett. 218 B (1989) 245.

Figure Captions:

Fig.1.

x-dependence of $\Delta g(x)/g(x)$ for different models of proton spin.

Fig.2(a).

Asymmetries using the parametrisation of Set 1 with $\nu = 70 - 190 GeV$ and $Q^2 = 0.1 - 20.0 GeV^2$

Fig.2 (b).

Asymmetries using the parametrisation of Set 2 with $\nu = 70 - 190 GeV$ and $Q^2 = 0.1 - 20.0 GeV^2$.

Fig. 2 (c).

Asymmetries using the parametrisation of Set 3 with $\nu = 70 - 190 GeV$ and $Q^2 = 0.1 - 20.0 GeV^2$.

Fig. 2 (d).

Asymmetries using the parametrisation of Set 4 with $\nu = 70 - 190 GeV$ and $Q^2 = 0.1 - 20.0 GeV^2$.

Fig. 3 (a).

Comparison of predictions of Set 1 (continuous line) and Set 3 (dashed line).

Fig. 3 (b).

Comparison of predictions of Set 1 (continuous line) and Set 4 (dashed line).

Fig. (4)

Asymmetry using Set I parametrisation for $\nu = 130 GeV$ and with a, α and N_g taken from Table 1.

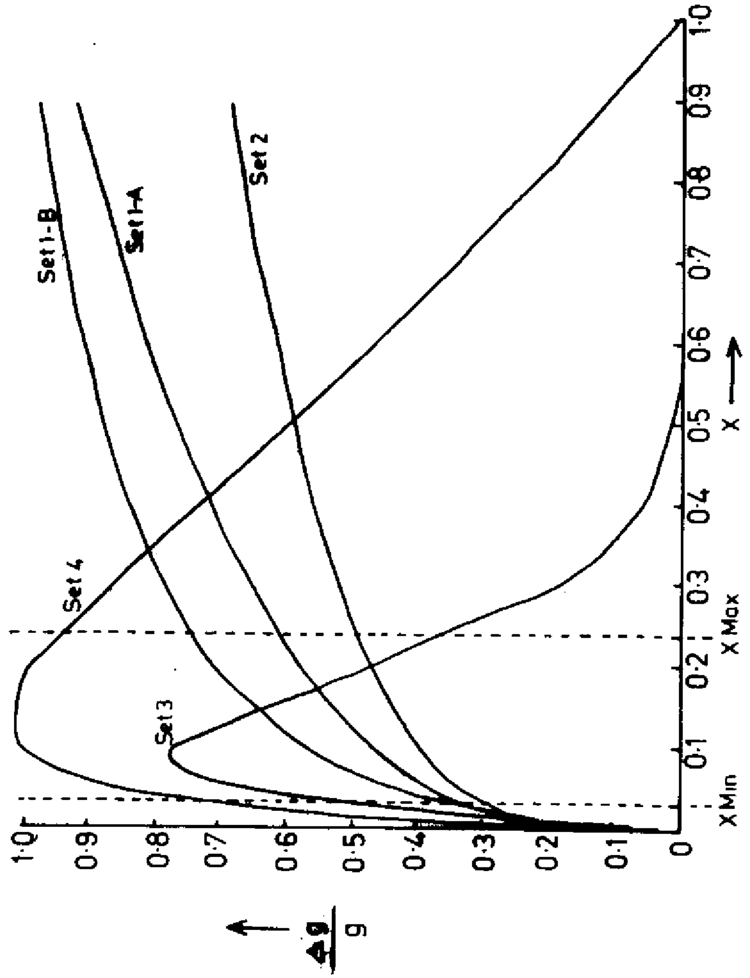

Fig.1

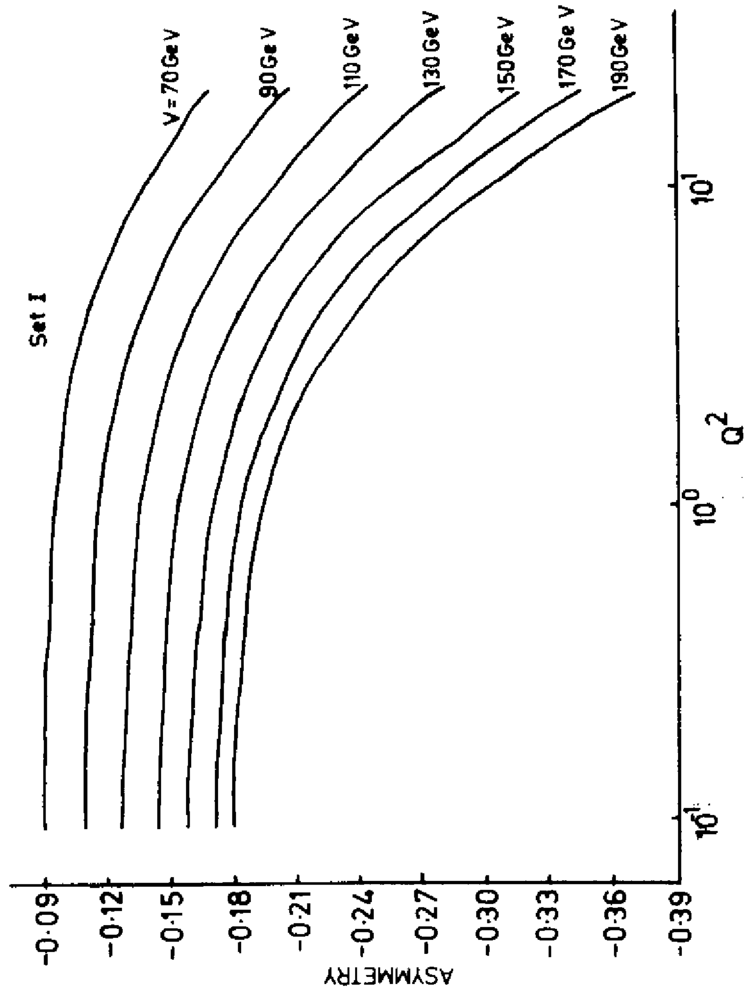

Set I
V=70 GeV
90 GeV
110 GeV
130 GeV
150 GeV
170 GeV
190 GeV
ASYMMETRY
-0·09
-0·12
-0·15
-0·18
-0·21
-0·24
-0·27
-0·30
-0·33
-0·36
-0·39
10^{-1}
10^{0}
10^{1}
Q^2

Fig.2(a)

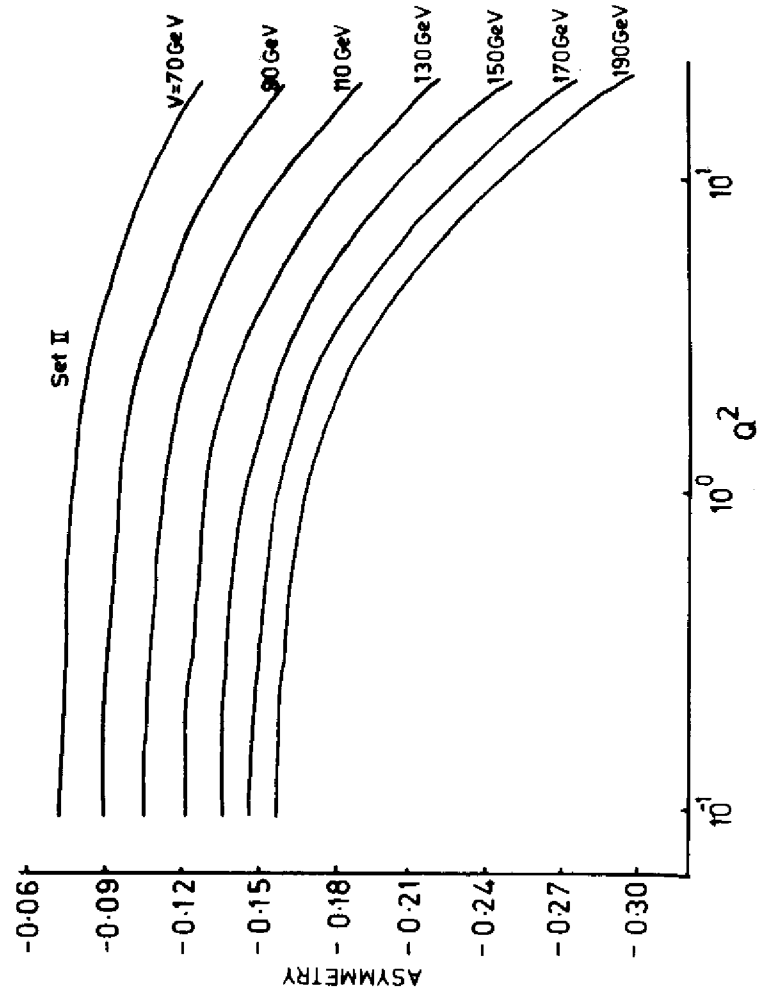

Set II
V=70 GeV
90 GeV
110 GeV
130 GeV
150 GeV
170 GeV
190 GeV
ASYMMETRY
-0·06
-0·09
-0·12
-0·15
-0·18
-0·21
-0·24
-0·27
-0·30
10^{-1}
10^{0}
10^{1}
Q^2

Fig.2(b)

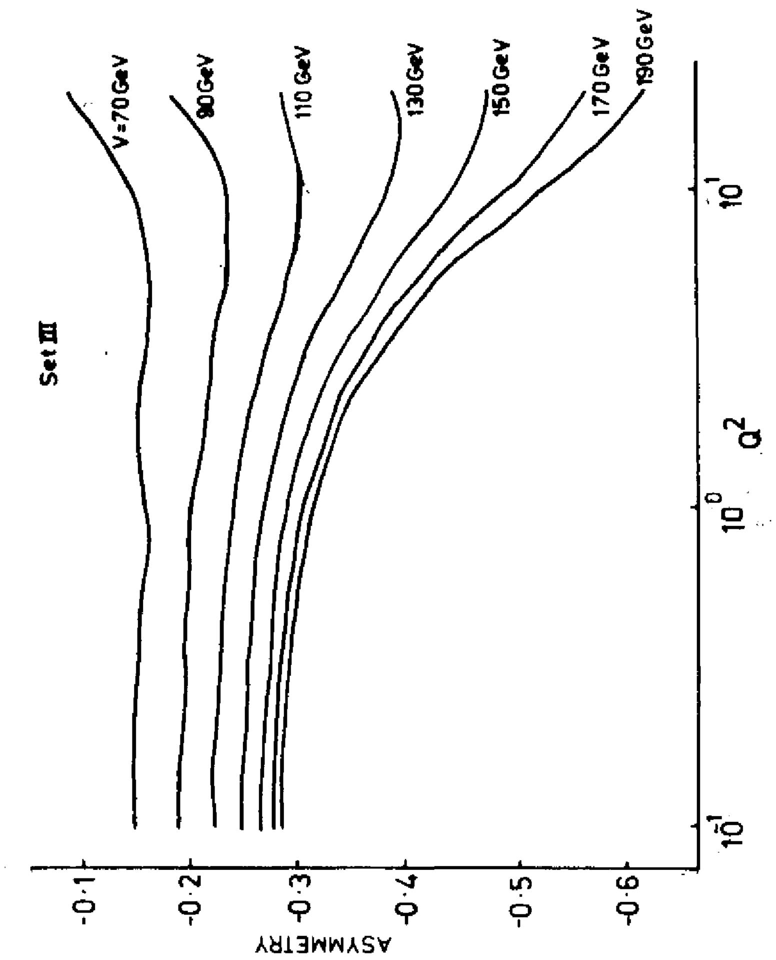
Set III
V=70GeV
90GeV
110 GeV
130GeV
150GeV
170GeV
190GeV
ASYMMETRY
-0·1
-0·2
-0·3
-0·4
-0·5
-0·6
10^{-1}
10^{0}
10^{1}
Q^2

Fig.2(c)

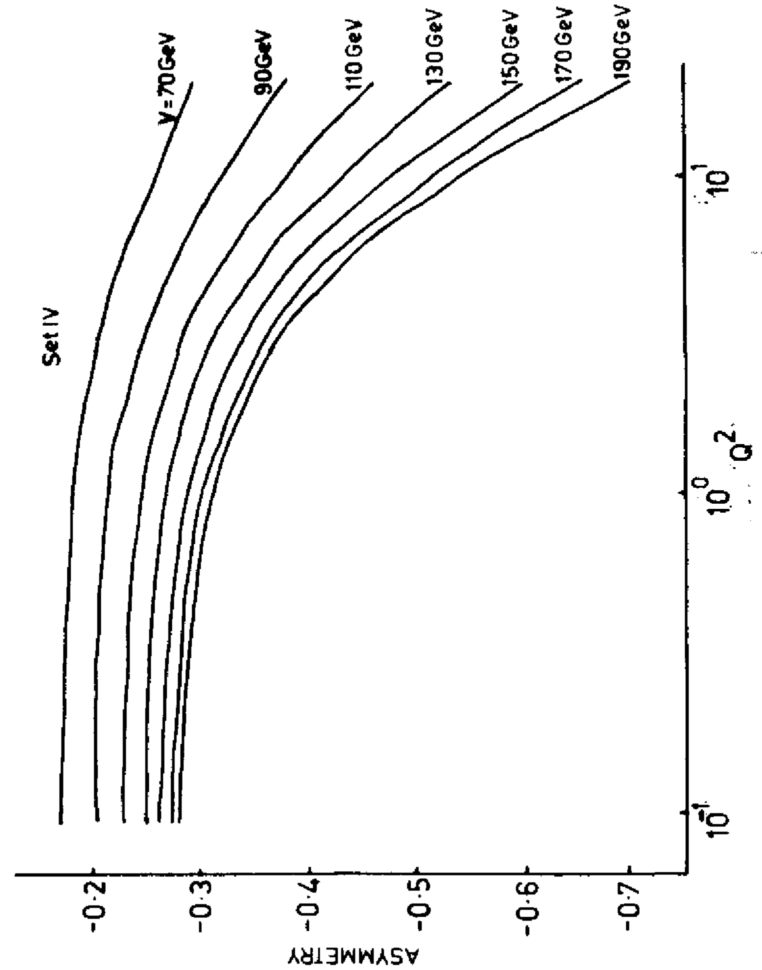
Set IV
V=70GeV
90GeV
110GeV
130GeV
150GeV
170GeV
190GeV
ASYMMETRY
-0·2
-0·3
-0·4
-0·5
-0·6
-0·7
10^{-1}
10^{0}
10^{1}
Q^2

Fig.2(d)

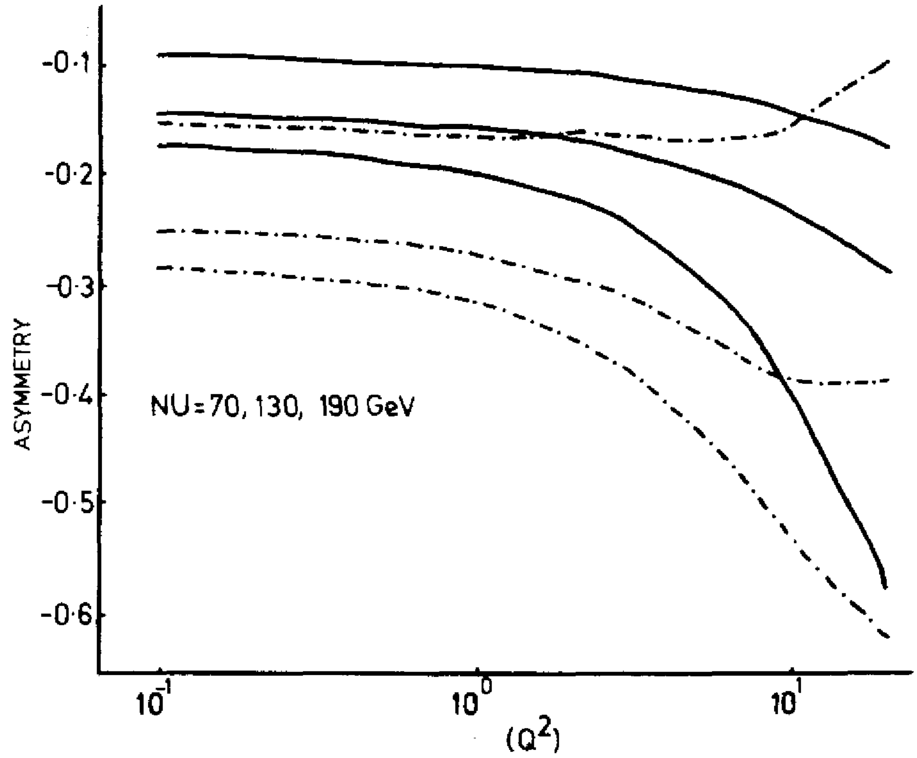
-0·1
-0·2
-0·3
-0·4
-0·5
-0·6
ASYMMETRY
NU=70, 130, 190 GeV
10^{-1}
10^{0}
10^{1}
(Q^2)

Fig.3(a)

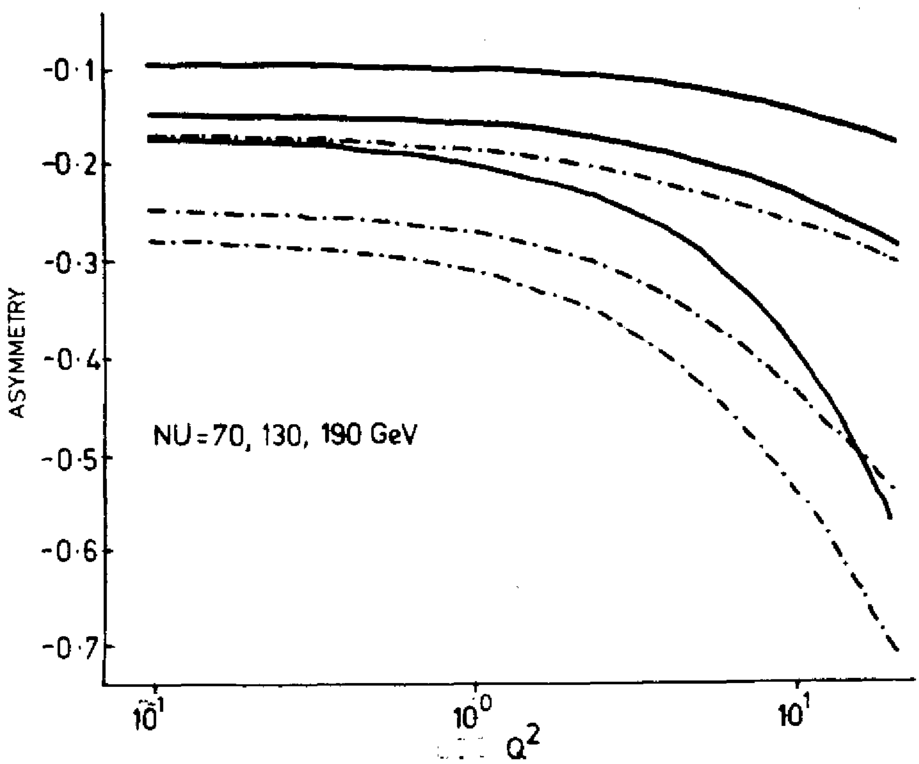
-0·1
-0·2
-0·3
-0·4
-0·5
-0·6
-0·7
ASYMMETRY
NU=70, 130, 190 GeV
10^{-1}
10^{0}
10^{1}
Q^2

Fig.3(b)

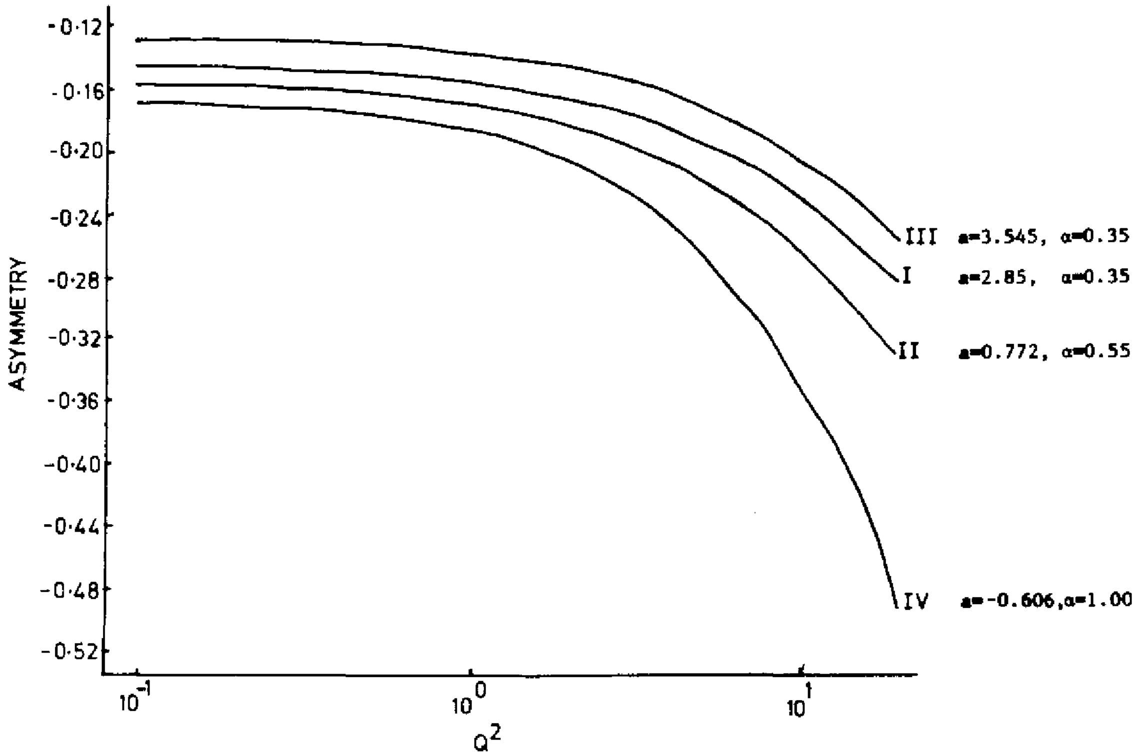
-0·12
-0·16
-0·20
-0·24
-0·28
-0·32
-0·36
-0·40
-0·44
-0·48
-0·52
ASYMMETRY
10^-1
10^0
10^1
Q^2
III a=3.545, α=0.35
I a=2.85, α=0.35
II a=0.772, α=0.55
IV a=-0.606,α=1.00

Fig.4

Stampato in proprio nella tipografia
del Centro Internazionale di Fisica Teorica